Available online at www.sciencedirect.com
ScienceDirect
Journal of Sound and Vibration 299 (2007) 22–35
JOURNAL OF SOUND AND VIBRATION
www.elsevier.com/locate/jsvi

Detection of fatigue cracks in a beam using a spatio-temporal dynamical system identification method

L.Z. Guo, S.A. Billings*

Department of Automatic Control and Systems Engineering, University of Sheffield, Sheffield S1 3JD, UK

Received 20 October 2005; received in revised form 16 June 2006; accepted 20 June 2006
Available online 11 September 2006

Abstract

The identification of fatigue cracks in a beam is investigated in this paper. It is shown that due to the influence of the elastic nonlinearity of fatigue cracks, the homogeneity, along the length of the beam, of the spatio-temporal dynamics of the vibrating beam is destroyed. By using spatio-temporal dynamical system identification techniques, a new approach is developed to detect this nonhomogeneity. The cracked beam is divided into several spatial regions and a coupled map lattice (CML) model is identified and verified in one of the regions using an orthogonal forward regression (OFR) least-squares algorithm. This CML model is then used to predict the dynamical behaviour of the other regions and in this way to detect the nonhomogeneity of the overall system.

1. Introduction

The detection and characterisation of fatigue cracks in a beam have been investigated over many years. Most of the techniques developed for this problem are based on vibration measurements and spectral analysis because it has been shown that sub- and super-harmonic resonance regimes, of a vibrating beam, are highly sensitive to the presence of fatigue cracks in structures ([1] and references therein). However, to apply the vibration-based methods, a mathematical model is generally needed. There have been considerable attempts to understand and model the dynamics of a vibrating cracked beam. Well-known models include the one-dimensional cracked beam model [2], breathing crack model [3], and bilinear oscillator model [4], etc. But all of the above models arise from mainly theoretical consideration and are derived by analytic modelling methods where often a large number of assumptions have to be made in order to obtain such models. For instance, there are several assumptions on the displacement, velocity and stress fields in the Christides and Barr [2] model. A pair of symmetric cracks is always assumed to remain open as the beam is vibrating so as to avoid the nonlinear characteristics of an opening and closing crack. It should be stressed that although some information about the physical properties for many of these systems might be available, normally not all the dynamical structures and parameters are known, therefore, the resulting theoretical models are often over-simplified, or even in error. These problems can result in large discrepancies between simulated and observed

*Corresponding author. Tel.: +44 114 2225232; fax: +44 114 2225661.
E-mail address: s.billings@sheffield.ac.uk (S.A. Billings).

0022-460X/$ - see front matter
doi:10.1016/j.jsv.2006.06.049

patterns both qualitatively and quantitatively. Therefore, there is a need to use identification methods to refine, update, validate, or even replace these theoretical models.

From a spatio-temporal dynamics point of view, the opening and closing of a crack not only causes the dynamical behaviour of the vibrating beam to be significantly nonlinear but also destroys the homogeneity, along the length of the beam, of the spatio-temporal dynamics because of the local decrease of the flexural rigidity of the damaged cross-section of the beam. The identification of homogeneous spatio-temporal dynamical systems has been studied by several researchers including Refs. [5–7]. The identification algorithms developed are mainly used to obtain a spatio-temporal model with both discrete space and time. These kind of models are generally called coupled map lattice (CML) models of spatio-temporal systems. It is well known that computer simulations have emerged as an effective and powerful tool to study complex spatio-temporal systems. In such cases the spatio-temporal dynamical systems by necessity are discretised in space as well as in time. This was one of the main motivations for the introduction of CML models of spatio-temporal systems. CML models were developed in the late 1980s and can exhibit surprisingly rich dynamical behaviours, including spatio-temporal chaos, intermittency, travelling waves and pattern formation [8–12]. CML's have been used to model convected temperature fluctuations in the atmosphere [13], boiling processes [14], spatio-temporal chaos in fluid flows [15] and cloud dynamics [16]. In this paper, a CML model will be used to model the dynamics of a fatigue-cracked beam in vibration using a nonhomogeneous spatio-temporal system identification method. The idea behind the proposed identification method is that the cracked beam is divided into several spatial regions and a CML model is identified and verified in one of the regions using an orthogonal forward regression (OFR) least-squares algorithm [17]. This CML model is then used to predict the dynamical behaviour of the other spatial regions and in this way to detect the nonhomogeneity of the overall system. The advantages of the proposed method are that an analytic mathematical model is not necessary and the method can be used in association with classical spectral analysis techniques which can provide more reliable crack detection results.

The paper is organised as follows. Section 2 presents a dynamic model of a fatigue-cracked beam which is used to generate data for this simulation study. The basic concept of CML models is introduced in Section 3. The nonhomogeneous spatio-temporal system identification algorithm for detecting the correct terms and determining the associated parameter estimates is presented in Section 4. Section 5 applies the proposed identification approach to the crack detection problem, and finally conclusions are given in Section 6.

2. Dynamic model of a fatigue-cracked beam

For the purpose of this numerical simulation study, a simplified dynamic model of the cracked beam is adapted from Tsyfansky and Beresnevich [18] to generate data. The beam under consideration, which is shown in Fig. 1, is a solid-spar homogeneous viscoelastic beam with a ratio of the length and the thickness around 20, which resists the greater part of an external load.

The dynamic model is defined by using a viscoelastic cantilever beam performing bending vibrations excited by a harmonic test force, $P\sin(\omega t)$

$$\frac{\partial^2}{\partial x^2}\left[EI(x)\frac{\partial^2 y}{\partial x^2}\right]+\mu(x)\frac{\partial^2 y}{\partial t^2}+\frac{\partial^2}{\partial x^2}\left[bEI(x)\frac{\partial^3 y}{\partial t\partial x^2}\right]=q(x,t), \tag{1}$$

where $EI(x)$ and $\mu(x)$ are the flexural rigidity in bending and the distributed mass, respectively, of the beam cross-section with coordinate x, y is the lateral displacement of the beam cross-section measured from the static equilibrium position, and b is the coefficient of internal friction. In this study, for the sake of simplicity b is set to be zero, that is internal friction is ignored, therefore Eq. (1) is simplified to be

$$\frac{\partial^2}{\partial x^2}\left[EI(x)\frac{\partial^2 y}{\partial x^2}\right]+\mu(x)\frac{\partial^2 y}{\partial t^2}=q(x,t). \tag{2}$$

The boundary conditions are

$$y(0,t)=0,\quad \frac{\partial y}{\partial x}(0,t)=0,\quad \frac{\partial^2 y}{\partial x^2}(l,t)=0,\quad \frac{\partial^3 y}{\partial x^3}(l,t)=0. \tag{3}$$

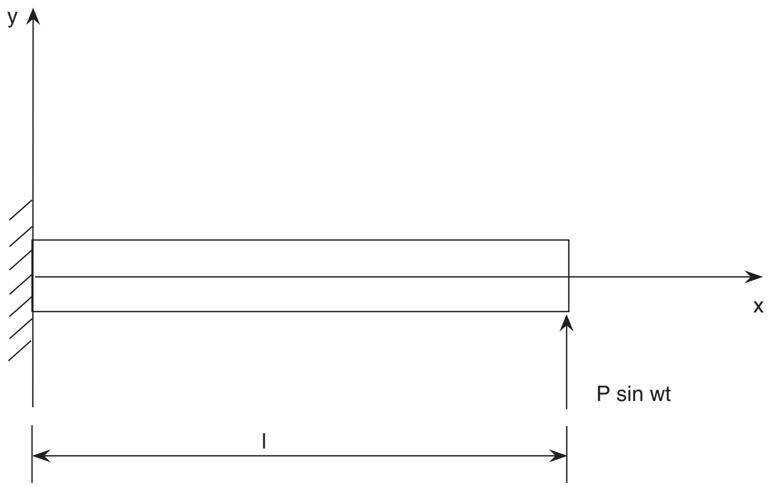

Fig. 1. Schematic diagram of the beam.

The first two boundary conditions mean the end 0 is restrained so that the displacement and slope vanish always. The last two boundary conditions indicate that the end l is free so that both curvature and shear are zero.

To model the fatigue crack in the beam, Tsyfansky and Beresnevich [18] consider a fatigue crack as an additional elastic nonlinearity describing the cyclical process of opening and closing of the crack edges during vibration and use a piecewise linear crack model. More specifically, this cyclical process is simulated using a crack parameter, σ. The parameter σ is a step function describing the relationship between the flexural rigidity of the damaged cross-section and the bend angle $\phi = \partial y/\partial x$. The mathematical form of this function is dependent on the location of the fatigue crack above or below the centreline along which x is measured.

In the case of an upper-half crack location the crack edges for the static equilibrium position of the system are initially opened due to the action of the beam's own weight. The crack parameter σ is described by the expression

$$\sigma = \begin{cases} 0, & \dfrac{\partial y}{\partial x} > \phi_0, \\ \sigma_c, & \dfrac{\partial y}{\partial x} \leqslant \phi_0, \end{cases} \tag{4}$$

where $\sigma_c = (1 - I_d/I_0)$ is a measure of the relative crack value, I_d being the second moment of the damaged cross-section, and I_0 is the second moment of the undamaged cross-section, ϕ_0 is the threshold value of the bend angle, ϕ, corresponding to the instant of closing (or opening) of the crack edges. Similarly, for a crack located in the lower-half of the beam, the crack parameter σ is calculated as

$$\sigma = \begin{cases} 0, & \dfrac{\partial y}{\partial x} \leqslant \phi_0, \\ \sigma_c, & \dfrac{\partial y}{\partial x} > \phi_0. \end{cases} \tag{5}$$

The crack parameter, σ, defines the change in flexural rigidity of the damaged cross-section $EI(x - x_d)$ in accordance with the following mathematical expression:

$$EI(x = x_d) = EI_0[1 - \sigma\delta(x - x_d)], \tag{6}$$

where EI_0 is the flexural rigidity in bending of the undamaged cross-section, and x_d is the coordinate of the damaged cross-section of the beam. The intensity of the distributed load $q(x, t)$ is given by

$$q(x, t) = P\,\sin(\omega t) \cdot \delta(x - x_p) - k(y - y_{\rm st}) \cdot \delta(x - x_k), \tag{7}$$

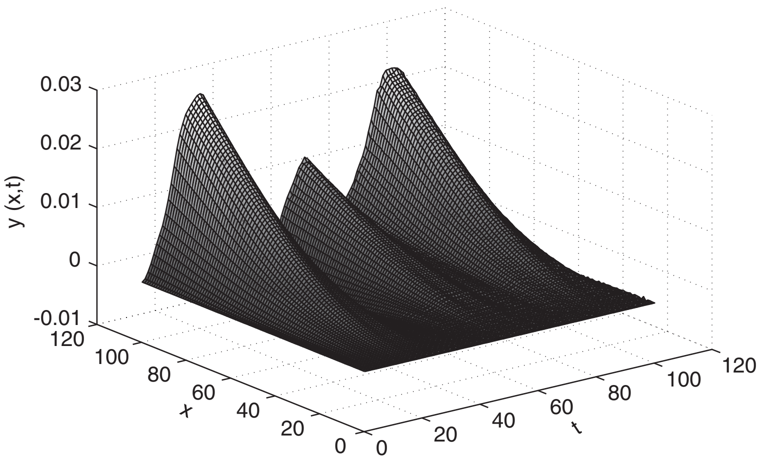

Fig. 2. The numerical solution of the fatigue-cracked beam.

where P and ω are the amplitude and the frequency of the external harmonic excitation, $\delta(x - x_p)$ is a Dirac delta function, and $x_p = l$ is the coordinate of the cross-section to which the external harmonic force is applied. l is the length of the beam. Note that the extra term inserted in Eq. (7) is considered as introducing an additional elastic support in the beam in order to balance the influence of the beam's own weight with the position of the bend point, $\phi = \phi_0$, of the damaged cross-section such that ϕ_0 can be set to be zero. k and y_{st} are the stiffness coefficient and the initial static deformation in compression of the additional elastic support, and $x_k = 0.9l$ is the coordinate of the cross-section when interacting with the additional elastic support.

The partial differential (2), subject to conditions (3)–(7) was numerically solved using a fourth-order Runge–Kutta method with spatial sampling interval 0.12 and time sampling interval 0.01 and it was assumed that the crack is located in the upper-half of the beam and the location of the crack was taken as $x_d = l/20$ with $l = 12\,\mathrm{m}$. The parameters used in the numerical algorithm were $EI(x) = 3.3903 \times 10^7\,\mathrm{N\,m^2}$, $\mu(x) = 1.9933 \times 10^2\,\mathrm{kg/m}$, $P = 0.2G$, where G is the weight of the beam, $\omega = 10$, $\sigma_c = 0.17$, $k = 1.0 \times 10^4$, $ky_{st}/G = 0.34$, and $\phi_0 = 0$. The data is shown in Fig. 2. A detailed analysis about the effects of a fatigue crack on the excitation of superharmonic responses in vibrating beam can be found in Ref. [18]. In this paper, a spatio-temporal identification method will be presented as an alternative method of crack detection problem.

3. The CML model

A CML model is a discrete space and time representation of spatio-temporal dynamic systems which is defined in a lattice as follows. Let I denote a d-dimensional lattice consisting of the set of all integer coordinate vectors $i = (i_1, \ldots, i_d) \in \mathbf{Z}^d$. The deterministic CML model of spatio-temporal dynamical systems defined over I is of the following form:

$$\begin{aligned} \mathbf{x}(t) &= f(\mathbf{x}(t-1), \mathbf{u}(t-1)), \\ \mathbf{y}(t) &= h(\mathbf{x}(t)), \end{aligned} \tag{8}$$

where $\mathbf{x}(t) = \{\mathbf{x}_i(t)\}_{i\in I} \in X = \prod_{i\in I} X_i, X_i \subset \mathbf{R}^n, \mathbf{y}(t) = \{\mathbf{y}_i(t)\}_{i\in I} \in Y = \prod_{i\in I} Y_i$, $Y_i \subset \mathbf{R}^l$, and $\mathbf{u}(t) = \{\mathbf{u}_i(t)\}_{i\in I} \in U = \prod_{i\in I} U_i \subset \mathbf{R}^m$, are the global state, output, and input, respectively. $f : X \times U \to X$ is a sequence of differentiable maps $f = \{f_i\}_{i\in I}$ and $h : X \to Y$ is a sequence of differentiable maps sequence $h = \{h_i\}_{i\in I}$.

The CML model (8) can also be written, in terms of the index of nodes, as follows

$$\begin{aligned} \mathbf{x}_i(t) &= f_i(\mathbf{x}_i(t-1), \mathbf{u}_i(t-1), \mathbf{s}^m\mathbf{x}_i(t-1), \mathbf{s}^m\mathbf{u}_i(t-1)), \\ \mathbf{y}_i(t) &= h_i(\mathbf{x}_i(t), \mathbf{s}^m\mathbf{x}_i(t-1)), \quad i \in I, \end{aligned} \tag{9}$$

where $\mathbf{x}_i(t) \in X_i \subset \mathbf{R}^n$, $\mathbf{y}_i(t) \in Y_i \subset \mathbf{R}^l$, and $\mathbf{u}_i(t) \in U_i \subset \mathbf{R}^m$, X_i, Y_i, and U_i are open sets, n, l, and m-dimensional vectors representing the local state, output, and input variables respectively at the ith node in I. $\mathbf{s}^m$ is a spatial shift operator, which is defined as

$$\mathbf{s}^m = (s^{p_1}, s^{p_2}, \ldots, s^{p_m}) \tag{10}$$

such that

$$\mathbf{s}^m \mathbf{x}_i(t) = (\mathbf{x}_{i+p_1}(t), \mathbf{x}_{i+p_2}(t), \ldots, \mathbf{x}_{i+p_m}(t)), \tag{11}$$

where $p_1, p_2, \ldots, p_m$ are the indices of the neighbours of the ith node—that is the region in I around the ith node, which influences the dynamics of that particular node.

Generally it is also assumed that the following input–output representation

$$\mathbf{y}_i(t) = g_i(\mathbf{q}^{n_y}\mathbf{y}_i(t), \mathbf{q}^{n_u}\mathbf{u}_i(t), \mathbf{s}^{m'}\mathbf{q}^{n_y}\mathbf{y}_i(t), \mathbf{s}^{m'}\mathbf{q}^{n_u}\mathbf{u}_i(t)) \tag{12}$$

can be derived for any site from Eq. (9). In Eq. (12), $\mathbf{q}$ is a backward shift operator such that

$$\mathbf{q}^{n_y}\mathbf{y}_i(t) = (\mathbf{y}_i(t-1), \mathbf{y}_i(t-2), \ldots, \mathbf{y}_i(t-n_y)). \tag{13}$$

Remark 1. In Eq. (12) $g_i, i \in I$ are generally nonlinear differentiable maps depending on the history of the local input and output variables, and on the variables at some neighbouring nodes. If $g_i, i \in I$ are unknown then the nonlinearity of g_i makes it difficult to apply traditional identification techniques. It is common practice to approximate nonlinear input–output equations from the available data using a known set of basis functions or regressors. Typical classes of regressors used in nonlinear identification include polynomial and rational functions, Gaussian radial basis functions and wavelets. In this paper, polynomials are chosen as basis functions to approximate the CML model (12).

Remark 2. It is worth noting that if $g_i = g_j$ for all $i, j \in I$, the CML model is considered to be spatially homogeneous and nonhomogeneous otherwise. As mentioned earlier, the identification problem of homogeneous spatio-temporal dynamic systems has been studied by several researchers. In this paper, the identification problem of nonhomogeneous spatio-temporal dynamic systems is considered and applied to the crack detection problem in structures.

Generally, a spatio-temporal dynamic system in the form of a partial differential equation can be discretised as a CML model. For instance, reconsider the partial differential (2), by approximating the spatial and time derivatives using a finite difference method and letting $x^{(1)}(x,t) = y(x,t)$, $x^{(2)}(x,t) = \partial y(x,t)/\partial t$, and $u(x,t) = q(x,t)$ system (2) can then be described as the following CML model:

$$\begin{aligned}
x_i^{(1)}(t) &= x_i^{(1)}(t-1) + Tx_i^{(2)}(t-1),\\
x_i^{(2)}(t) &= x_i^{(2)}(t-1) + \frac{T}{\mu_i}u_i(t-1) - \frac{T}{h^4\mu_i}(EI_{i+1}x_{i+2}^{(1)}(t-1) - 2(EI_{i+1} + EI_i)x_{i+1}^{(1)}(t-1)\\
&\quad + (EI_{i+1} + 4EI_i + EI_{i-1})x_i^{(1)}(t-1) - 2(EI_i + EI_{i-1})x_{i-1}^{(1)}(t-1)\\
&\quad - 2(EI_i - EI_{i-1})x_{i-2}^{(1)}(t-1)),\\
y_i(t) &= x_i^{(1)}(t),
\end{aligned} \tag{14}$$

where $x_i^{(1)}(t) = y(x_i, t)$, $x_i^{(2)}(t) = \dot{y}(x_i, t)$, $h = x_i - x_{i-1}$, $i = 1, \ldots, M$, and T is the time sampling interval.

Obviously this is a nonhomogeneous spatio-temporal system because the damaged cross-section makes the flexural rigidity $EI(x)$ non-uniform along the length of the beam.

4. Identification approach

The identification of CML models of homogeneous spatio-temporal dynamic systems can generally be obtained using data from one single node and its neighbours. This is because the underlying system is assumed to be homogeneous and all the dynamics at all the nodes are the same. Although the model structures or parameters are different in the case when the underlying system is nonhomogeneous, in principle, the identification of such nonhomogeneous spatio-temporal dynamic systems can be conducted by applying an identification algorithm to every single node in the overall lattice. However, this will often be a formidable task because the size of the lattice maybe very high. For instance, a two-dimensional lattice of size 100×100 contains 10,000 nodes. This means that a total of 10,000 CML models would need to be identified. On the other hand, there may only be a few nodes that appear to be nonhomogeneous such as for example in a uniform beam with one or several fatigue cracks. In this case it is not necessary to identify a single CML model for each single node in the lattice. In this paper, a strategy is proposed to solve this problem. The basic idea behind the approach is that the lattice is initially divided into several regions, say two or three, and a CML model is then identified and validated using the observations from one of the regions. This identified CML model is then used to predict the dynamic response of the other regions and the predicted results may be "good" or "bad" depending on which region is used. If the dynamics in a region is the same as that in the region used for identification, then the identified and validated model should be able to produce good predictions. If the prediction results are not acceptable in some region, this may indicate that nonhomogeneity may have occurred in this particular region. This "bad" region can then be refined, that is, divided into smaller subregions before the strategy is repeated until all the dynamics of this nonhomogeneous system are obtained.

Assume that the maps $g_i, i \in I$ in Eq. (12) are all unknown and to be identified. Let $\Omega \subset I$ be a subarea of the lattice I. The identification problem of $g_i, i \in \Omega$ can be stated as follows.

Given observations $y_i(t-1), \ldots, y_i(t-n_y)$, $u_i(t-1), \ldots, u_i(t-n_u)$, and $\mathbf{s}^{m'}\mathbf{q}^{n_y}y_i(t), \mathbf{s}^{m'}\mathbf{q}^{n_u}u_i(t), i \in \Omega$, the objective of CML identification is to approximate the input–output relationship function g_i from these observations. Here it is assumed that y_i and u_i are one-dimensional variables for the sake of clarity. In this paper, the algorithm and results for CML identification using polynomials are presented.

Let $\boldsymbol{\alpha} = (\alpha_1, \ldots, \alpha_n)$ be a multi-index, that is an n-tuple of nonnegative integers α_k, and denote by $\mathbf{z}^{\boldsymbol{\alpha}}$ the monomial $z_1^{\alpha_1} \ldots z_n^{\alpha_n}$, which has degree $|\boldsymbol{\alpha}| = \sum_{k=1}^{n} \alpha_k$. Let s be a positive integer, and let $\Lambda = \{\boldsymbol{\alpha} \,|\, |\boldsymbol{\alpha}| < s\}$ a set of multi-indices, then the set of polynomials of total order s is $\Sigma_s = \mathrm{span}\{\mathbf{z}^{\boldsymbol{\alpha}} \,|\, |\boldsymbol{\alpha}| < s\}$. Note that Σ_s is a L-dimensional space, where $L = 1 + n + (n+1)n/2! + \cdots + (n+s-1)\cdots(n+1)n/s!$. Approximating nonlinear function g_i in Eq. (12) using the polynomial approximation space Σ_s yields the following representation:

$$y_i(t) = \theta_0 + \sum_{i_1=1}^{n} \theta_{i_1} z_{i_1}(t) + \sum_{i_1=1}^{n} \sum_{i_2=i_1}^{n} \theta_{i_1 i_2} z_{i_1}(t) z_{i_2}(t) + \cdots + \sum_{i_1=1}^{n} \cdots \sum_{i_s=i_s-1}^{n} \theta_{i_1 \ldots i_s} z_{i_1} \ldots z_{i_s} + \varepsilon(t), \tag{15}$$

where all θ represent polynomial coefficients and all $z(t)$ represent lagged terms in y_i, u_i, and their corresponding neighbours, and $\varepsilon(t)$ denotes the error of this representation. Given the representation (15), the objective of the identification algorithm is to select the significant terms from this set while estimating the corresponding monomial coefficients. In this paper, an orthogonal forward regression algorithm (OFR) [19] is employed. The OFR algorithm involves a stepwise orthogonalisation of the regressors and a forward selection of the relevant terms based on the error reduction ratio (ERR) criterion [17]. The algorithm provides the optimal least-squares estimate of the polynomial coefficients θ.

For a given candidate regressor set $G = \{\boldsymbol{\varphi}_m\}_{m=1}^{M}$, the OFR algorithm can be summarised as follows:

Step 1:

$$I_1 = I_M = \{1, \ldots, M\},$$
$$\mathbf{w}_m = \boldsymbol{\varphi}_m, \hat{b}_m = \frac{\mathbf{w}_m^{\mathrm{T}}\mathbf{y}}{\mathbf{w}_m^{\mathrm{T}}\mathbf{w}_m}, \tag{16}$$

$$l_1 = \arg\max_{m \in I_1} \left(\hat{b}_m^2 \frac{\mathbf{w}_m^{\mathrm{T}}\mathbf{y}}{\mathbf{y}^{\mathrm{T}}\mathbf{y}} \right) = \arg\max_{m \in I_1} (\mathrm{err}_m), \tag{17}$$

$$\mathbf{w}_1^0 = \mathbf{w}_{l_1}, \quad c_1^0 = \frac{\mathbf{w}_1^{0\mathrm{T}}\mathbf{y}}{\mathbf{w}_1^{0\mathrm{T}}\mathbf{w}_1^0}, \tag{18}$$

$$a_{1,1} = 1. \tag{19}$$

Step $j, j>1$:

$$I_j = I_{j-1} \backslash l_j - 1, \tag{20}$$

$$\mathbf{w}_m = \boldsymbol{\varphi}_m - \sum_{k=1}^{j-1} \frac{\mathbf{w}_k^{0\mathrm{T}} \mathbf{y}}{\mathbf{w}_k^{0\mathrm{T}} \mathbf{w}_k^0} \mathbf{w}_k^0, \quad \hat{b}_m = \frac{\mathbf{w}_m^{\mathrm{T}} \mathbf{y}}{\mathbf{w}_m^{\mathrm{T}} \mathbf{w}_m}, \tag{21}$$

$$l_j = \arg \max_{m \in I_j} \left(\hat{b}_m^2 \frac{\mathbf{w}_m^{\mathrm{T}} \mathbf{y}}{\mathbf{y}^{\mathrm{T}} \mathbf{y}} \right) = \arg \max_{m \in I_j} (\mathrm{err}_m), \tag{22}$$

$$\mathbf{w}_j^0 = \mathbf{w}_{l_j}, \quad c_j^0 = \frac{\mathbf{w}_j^{0\mathrm{T}} \mathbf{y}}{\mathbf{w}_j^{0\mathrm{T}} \mathbf{w}_j^0}, \tag{23}$$

$$a_{k,j} = \frac{\mathbf{w}_k^{0\mathrm{T}} \boldsymbol{\varphi}_{l_j}}{\mathbf{w}_k^{0\mathrm{T}} \mathbf{w}_k^0}, \quad k = 1, \ldots, j-1. \tag{24}$$

The procedure is terminated at the M_sth step when the termination criterion

$$1 - \sum_{m=1}^{M_s} \mathrm{err}_m < \rho \tag{25}$$

is met, where ρ is a designated error tolerance, or when a given number of terms in the final model is reached.

The estimated coefficients are calculated from the following equation:

$$\begin{pmatrix} \theta_{l_1} \\ \theta_{l_2} \\ \vdots \\ \theta_{l_{M_s}} \end{pmatrix} = \begin{pmatrix} 1 & a_{1,2} & \ldots & a_{1,M_s} \\ 0 & 1 & \vdots & a_{2,M_s} \\ \vdots & \vdots & \ddots & \vdots \\ 0 & 0 & \ldots & 1 \end{pmatrix}^{-1} \begin{pmatrix} c_1^0 \\ c_2^0 \\ \vdots \\ c_{M_s}^0 \end{pmatrix} \tag{26}$$

and the selected terms are $\varphi_{l_1}, \ldots, \varphi_{l_{M_s}}$.

Based on the algorithm, the iterative identification procedure for nonhomogeneous spatio-temporal systems can be outlined as follows

Step 1: Divide the spatial domain into several subregions and choose one of the regions for CML identification.

Step 2: Determine the spatial neighbourhood sites (represented by $\mathbf{s}^{m'}$) of the ith site in the selected subregion.

Step 3: Select the time lags n_y and n_u, then the process variables involved in the identification are

$$\{\mathbf{s}^{m'} y_i(t-1), \ldots, \mathbf{s}^{m'} y_i(t-n_y), \mathbf{s}^{m'} u_i(t-1), \ldots, \mathbf{s}^{m'} u_i(t-n_u)\}. \tag{27}$$

Step 4: Apply the orthogonal least-squares algorithm to obtain the terms and parameters of the CML model.

Step 5: Apply model validity tests to evaluate the model. If no valid models are found, then the set of candidate terms is refined with a higher polynomial degree to the set of candidate terms.

Step 6: Apply the obtained and validated CML model to other subregions to predict the dynamic responses in these subregions.

Step 7: Check the predicted errors for each subregion to detect the nonhomogeneous subregions. Select one of these subregions, go back to Step 1 and repeat the above procedure until all the dynamics have been identified.

Remark 3. The final model and parameters need to be assessed. A commonly used approach to check the validity of the identified model is to use higher-order statistical correlation analysis [20,21].

Remark 4. Note that in the above identification procedure, the spatial neighbourhood sites (represented by $\mathbf{s}^{m'}$) of the identified site and the time lags (n_y, n_u) need to be known a priori. In other words, the neighbourhood of the identified site, that is, the region around that site which influences the dynamics of that site in the spatial domain and the time domain need to be known before starting the identification. In practice, these two factors are important in determining the spatio-temporal dynamics of the underlying system. This problem is related to the embedding dimension problem in system reconstruction theory [22].

5. Applications to crack detection and analysis of results

To apply the proposed nonhomogeneous spatio-temporal system identification method, the spatial domain was sampled with a sampling interval 0.12 so that the number of nodes was 101. These 101 nodes were divided into two parts along the length of the beam corresponding to the two sections from 0 to 6 m and 6 to 12 m for a total length of the beam $l = 12$ m, respectively. Note that the location of the damaged cross-section is $l/20 = 0.6$ m which corresponds the node $i = 6$ and lies in the first part. Considering that an external force was applied at the far end of the beam which is located in the second area, the second area was used to identify a CML model for this spatio-temporal dynamics in this region. The data for identification was generated randomly in the subregion. Because the external force is only applied to the node $i = 99$ (here the node $i = 100$ and 101 are considered as boundary nodes), the identification data must include the data from the node $i = 99$. With the output and input lags set to be 3 and the neighbourhood set to be $i-2$, $i-1$, $i+1$, and $i+2$ it can be recognised that the considered input variables for the algorithm are polynomial combinations of $y_i(t-1), y_i(t-2), y_i(t-3), u_i(t-1), u_i(t-2), u_i(t-3), y_{i-1}(t-1), y_{i-1}(t-2), y_{i-1}(t-3), y_{i+1}(t-1), y_{i+1}(t-2), y_{i+1}(t-3), y_{i-2}(t-1), y_{i-2}(t-2), y_{i-2}(t-3), y_{i+2}(t-1), y_{i+2}(t-2), y_{i+2}(t-3)$. The identified model is listed in Table 1, where ERR denotes the error reduction ratio.

Table 1 shows that the obtained input–output representation at node i is

$$\begin{aligned} y_i(t) = {} & 0.0002228 + 2.2067y_i(t-1) - 1.2335y_i(t-2) + 0.00000010685u_i(t-1) \\ & - 0.000000079296u_i(t-2) + 0.20214y_{i+1}(t-1) - 0.13099y_{i+1}(t-2) + 0.040859y_{i+1}(t-3) \\ & - 0.33404y_{i+2}(t-1) + 0.14812y_{i+2}(t-2) + 0.079581y_{i+2}(t-3). \end{aligned} \tag{28}$$

The one-step-ahead predicted output and associated error for all the beam, that is both regions of the beam are shown in Figs. 3 and 4. A two-dimensional plane view (see Figs. 5 and 6) of the errors clearly indicates there are large predicted errors between nodes 3 and 10. It can be observed that the one-step-ahead predicted error falls between 0.001 and −0.0015 for the first subregion and 0.001 and −0.001 for the second subregion. Figs. 7–10 show the mean values, the ratio between the standard deviations of the one-step-ahead predicted error and the mean values of the output, the standard deviations of the output, and the ratio between the standard deviations of the one-step-ahead predicted error and the standard deviations of the output. From these figures, it can be seen that from node 10 to node 99 the standard deviations of the one-step-ahead predicted error are very small and are close to zero whilst they are quite large for the nodes between 3 and 10. All these observations confirm the existence of fatigue cracks in this spatio-temporal dynamic system and that

Table 1
The terms and parameters of the final CML model

Terms	Estimates	ERR
$y_i(t-1)$	2.2067e + 00	9.8740e − 01
$y_i(t-2)$	−1.2335e + 00	1.1585e − 02
Constant	2.2280e − 04	1.4261e − 04
$y_{i+2}(t-1)$	−3.3404e − 01	1.3888e − 04
$y_{i+2}(t-2)$	1.4812e − 01	2.0796e − 05
$u_i(t-1)$	1.0685e − 07	1.7473e − 05
$y_{i+1}(t-1)$	2.0214e − 01	1.3456e − 05
$y_{i+2}(t-3)$	7.9581e − 02	1.2724e − 05
$y_{i+1}(t-2)$	−1.3099e − 01	6.9377e − 06
$y_{i+1}(t-3)$	4.0859e − 02	1.5818e − 06
$u_i(t-2)$	−7.9296e − 08	1.0959e − 06

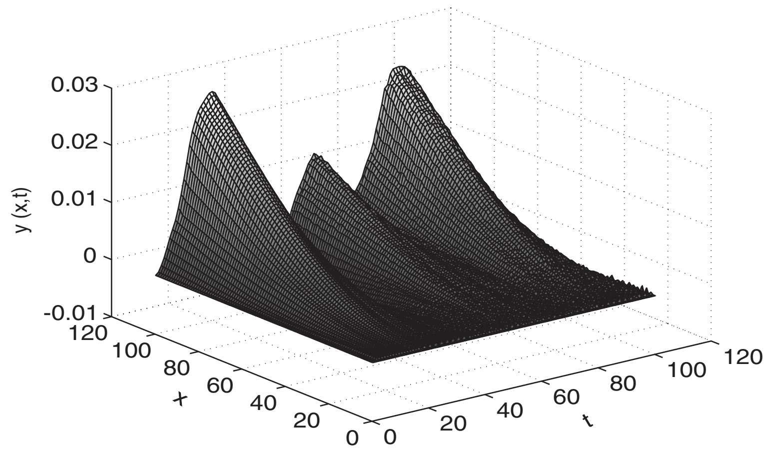

Fig. 3. One-step-ahead predicted output of the fatigue-cracked beam using the identified CML model over all the beam.

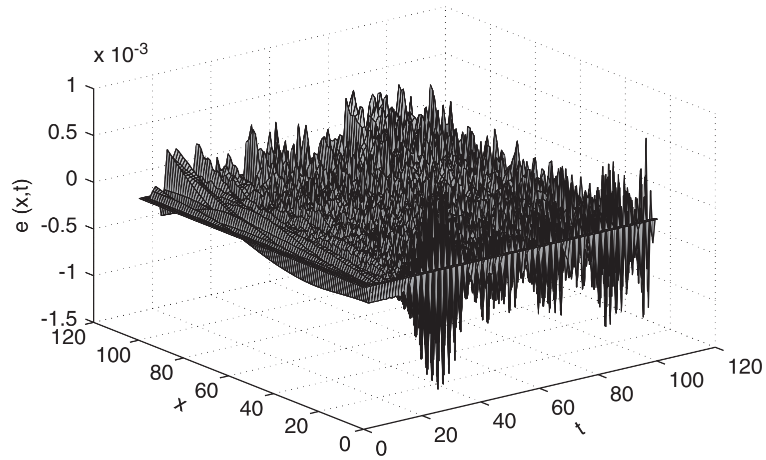

Fig. 4. One-step-ahead predicted error for model (28) over all the beam.

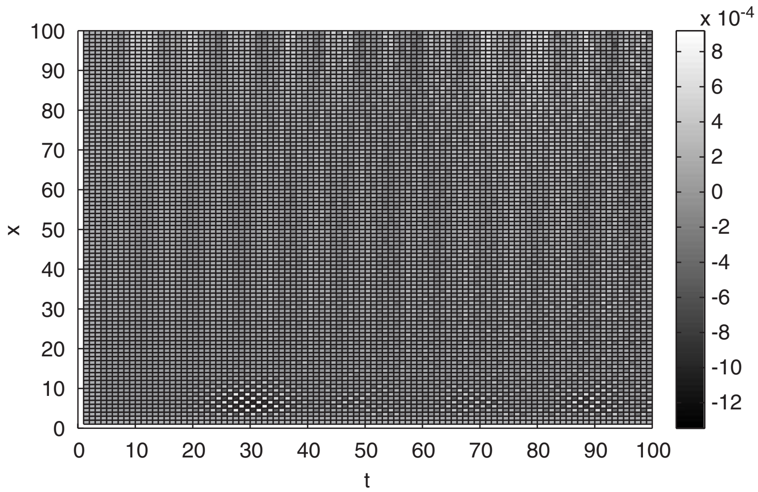

Fig. 5. Two-dimensional plane view of one-step-ahead predicted error for model (28) over all the beam.

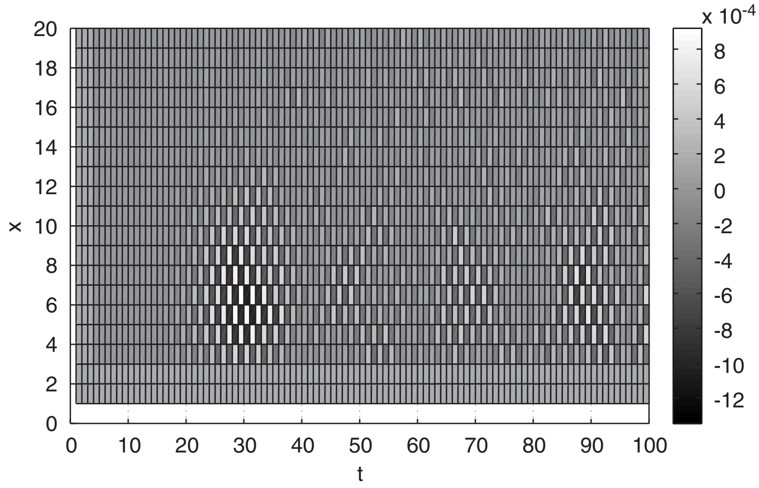

Fig. 6. Two-dimensional plane view of the one-step-ahead predicted error around the damaged cross-section $x_d = 0.6\,\text{m}$.

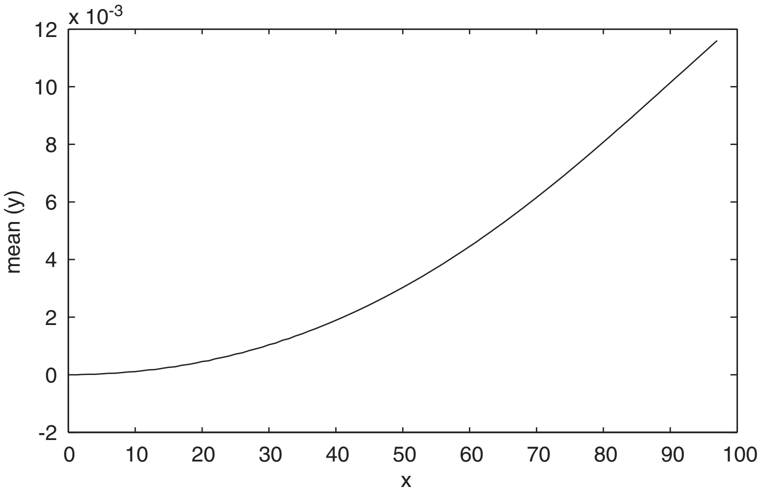

Fig. 7. Mean values of the output vs. the length of the beam.

this lies just between nodes $i = 3$ and 10 which corresponds to the section between 0.36 and 1.12 m along the length of the beam.

In order to obtain a CML model for the damaged area, that is the area between 0 and 1.12 m, the proposed identification algorithm was applied again to the data from this area. The obtained CML model is listed in Table 2. The one-step-ahead predicted error of this CML model for the crack-affected area, which falls in between 0.0004 and −0.0004, is plotted in Fig. 11.

From Table 2, it can be seen that the obtained input–output representation at node i in the crack-affected area is

$$\begin{aligned} y_i(t) = {} & 0.40331 y_{i+1}(t-1) + 0.56505 y_{i-1}(t-1) - 0.41632 y_i(t-3) y_{i-2}(t-2) \\ & + 0.61025 y_i(t-1) y_{i+2}(t-1) - 0.57826 y_i(t-3) y_{i+2}(t-3) + 0.53877 y_{i-2}(t-1) y_{i+1}(t-1) \\ & - 0.52157 y_i(t-3) y_{i-2}(t-3) + 0.58352 y_{i-1}(t-2) y_{i+1}(t-2) + 0.17437 y_{i+2}(t-2) \\ & + 0.22286 y_{i-1}(t-3) y_{i+1}(t-3). \end{aligned} \tag{29}$$

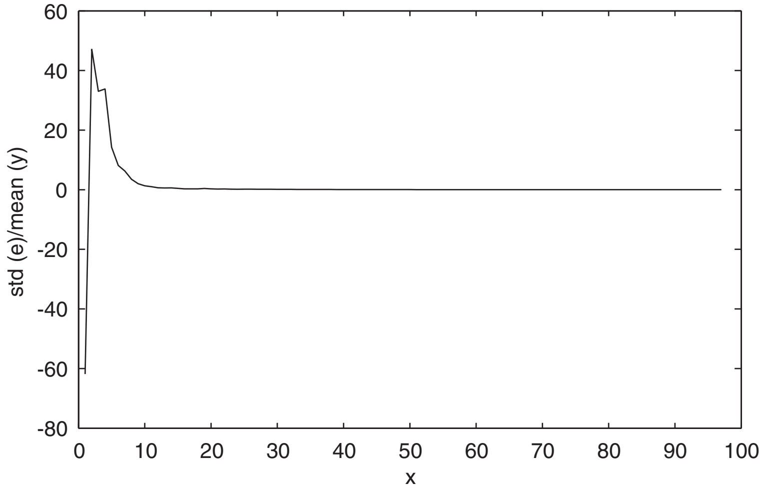

Fig. 8. The ratio between the standard deviations of the one-step-ahead predicted error and the mean values of the output vs. the length of the beam.

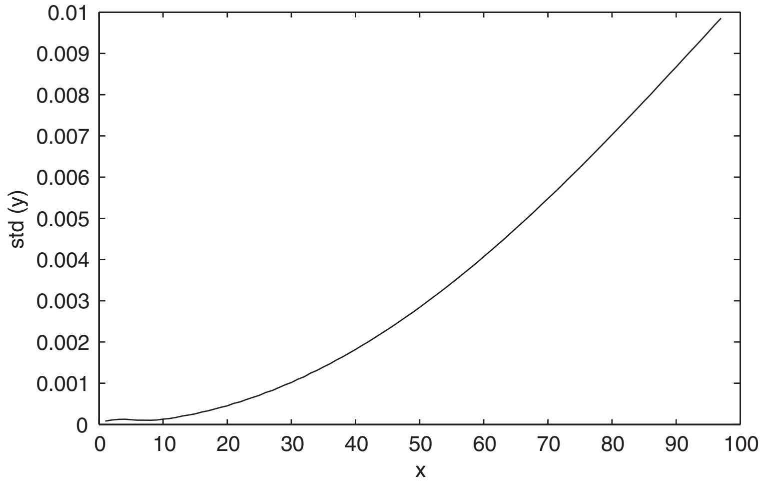

Fig. 9. The standard deviations of the output vs. the length of the beam.

The above results show that the identified CML models (28) and (29) together provide an excellent dynamical representation for the cracked beam in vibration.

Remark 5. The processes of dividing the lattice into subregions can be performed repeatedly to the predicted bad regions until the exact crack location is finally determined. In this paper, the beam is not divided any further just because the predicted results using one-step-bisection clearly indicate the location of the crack along the beam.

Remark 6. One of the advantages of the proposed approach is that the only quantity needs to be measured is the lateral displacement of the beam cross-section measured from the static equilibrium position as can be seen in Eqs. (28) and (29). In practice, the lateral displacements along the beam cross-sections can be easily measured by setting up several sensors along the beam.

Remark 7. Crack detection on a beam by the proposed method in this paper may be performed by the following operational procedure

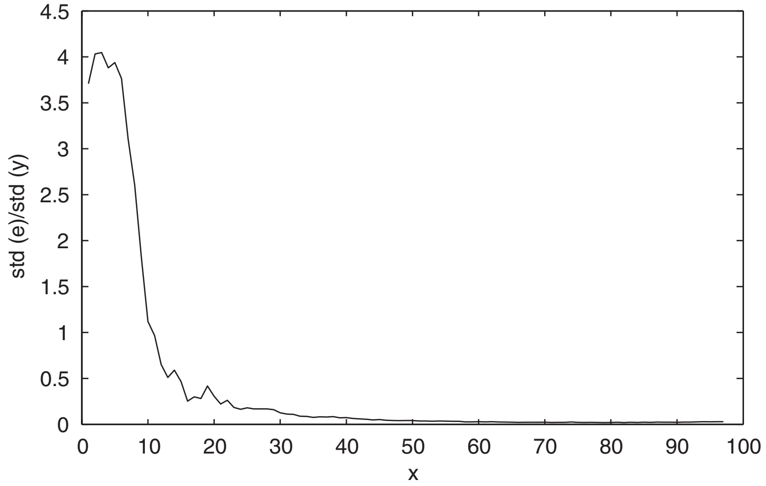

Fig. 10. The ratio between the standard deviations of the one-step-ahead predicted error and the standard deviations of the output vs. the length of the beam.

Table 2
The terms and parameters of the final CML model for the crack-affected area

Terms	Estimates	ERR
$y_{i+1}(t-1)$	4.0331e − 01	9.9935e − 01
$y_{i-1}(t-1)$	5.6505e − 01	2.6809e − 04
$y_i(t-3)y_{i-2}(t-2)$	−4.1632e − 01	3.4129e − 05
$y_i(t-1)y_{i+2}(t-1)$	6.1025e − 01	3.1586e − 05
$y_i(t-3)y_{i+2}(t-3)$	−5.7826e − 01	1.9373e − 05
$y_{i-2}(t-1)y_{i+1}(t-1)$	5.3877e − 01	9.5245e − 06
$y_i(t-3)y_{i-2}(t-3)$	−5.2157e − 01	9.4620e − 06
$y_{i-1}(t-2)y_{i+1}(t-2)$	5.8352e − 01	8.4744e − 06
$y_{i+2}(t-2)$	1.7437e − 01	7.4490e − 06
$y_{i-1}(t-3)y_{i+1}(t-3)$	2.2286e − 01	3.2115e − 06

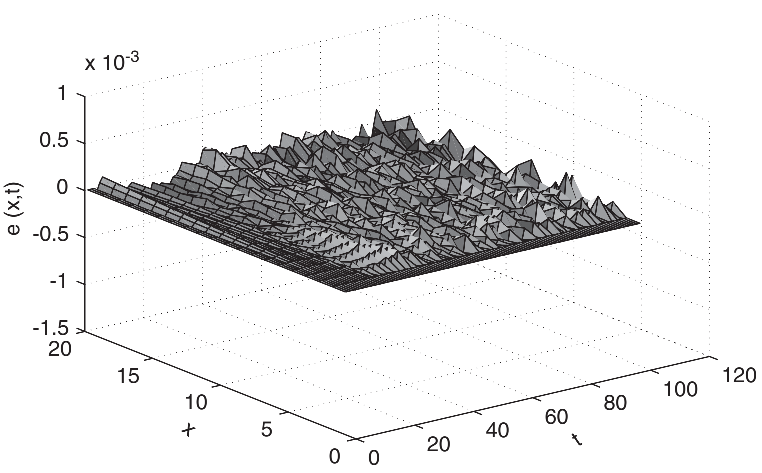

Fig. 11. One-step-ahead predicted error of the CML model for the crack-affected area.

- *Data (displacement $y_i(t)$) acquirement*: This can be done by installing sensors evenly distributed along the length of the whole beam and mounting the elastic support at the free end of the beam without any preliminary compression or extension. The forced bending vibrations of the test beam are then excited at some frequency (such as a frequency which is three times smaller than the first natural frequency of the system, suggested by Ref. [18]) while the lateral displacement of the beam cross-section is measured from the static equilibrium position.
- *Region division and CML identification*: The region division process can be implemented in a coarse-to-fine manner. Initially the beam can be divided into two subregions using a bisection method or a golden section method. Then the proposed spatio-temporal identification method is applied to one of the subregions to obtain a CML model.
- *Model prediction and analysis*: Validate the CML model and predict the system output for the other regions using the obtained CML model. Analyse the predicted errors and determine the bad subregions and subdivide the bad region into subregions and apply the identification method again until the position of the crack is determined.

Additionally, the proposed spatio-temporal identification method may be used associated with other methods such as the super-resonant vibration method [18].

6. Conclusions

An identification method for CML models of nonhomogeneous spatio-temporal dynamic systems has been proposed and applied to the crack detection problem in structures. The new method extends identification techniques for homogeneous systems in such a way that the identification algorithm can be applied in a coarse-to-fine manner so that the nonhomogeneity of the system can be detected. It has been shown by simulation that the proposed method cannot only effectively detect cracks in a beam but also generates an excellent CML model representation for the spatio-temporal dynamics of the vibrating beam.

Acknowledgement

The authors gratefully acknowledge financial support from EPSRC (UK).

References

[1] A.P. Bovsunovsky, C. Surace, Considerations regarding superharmonic vibrations of a cracked beam and the variation in damping caused by the presence of the crack, *Journal of Sound and Vibration* 288 (2005) 865–886.
[2] S. Christides, A.D.S. Barr, One-dimensional theory of cracked Bernoulli–Euler beam, *Journal of Mechanical Sciences* 26 (1984) 639–648.
[3] M.-H.H. Shen, Y.C. Chu, Vibrations of beams with a fatigue crack, *Computers and Structures* 45 (1992) 79–93.
[4] Y.C. Chu, M.-H.H. Shen, Analysis of forced bilinear oscillators and the application to cracked beam dynamics, *American Institute of Aeronautics and Astronautics* 30 (1992) 2512–2519.
[5] D. Coca, S.A. Billings, Identification of coupled map lattice models of complex spatio-temporal pattern, *Physics Letters A* 287 (2001) 65–73.
[6] S.A. Billings, D. Coca, Identification of coupled map lattice models of deterministic distributed parameter systems, *International Journal of Systems Science* 33 (2002) 623–634.
[7] S.A. Billings, L.Z. Guo, H.L. Wei, Identification of coupled map lattice models for spatio-temporal patterns using wavelets, *International Journal of Systems Science* (2006), to appear.
[8] K. Kaneko, Spatio-temporal intermittency in couple map lattices, *Progress of Theoretical Physics* 74 (1985) 1033–1044.
[9] K. Kaneko, Tuebulence in coupled map lattices, *Physica D* 18 (1986) 475–476.
[10] K. Kaneko, Spatiotemporal chaos in one- and two-dimensional coupled map lattices, *Physica D* 37 (1989) 60–82.
[11] K. Kaneko, Pattern dynamics in spatiotemporal chaos: pattern selection, diffusion of defect and pattern competition intermittency, *Physica D* 34 (1989) 1–41.
[12] K. Kaneko (Eds.), *Coupled Map Lattice: Theory and Experiment*, World Scientific, Singapore, 1993.
[13] N. Platt, S. Hammel, Pattern formation in driven coupled map lattices, *Physica A* 239 (1997) 296–303.
[14] T. Yanagita, Phenomenology of boiling: a coupled map lattice model, *Chaos* 2 (1992) 343–350.
[15] G. He, L. Cao, J. Li, Convective coupled map for simulating spatiotemporal chaos in flows, *Acta Mechanica Sinica* 11 (1995) 1–7.

[16] T. Yanagita, K. Kaneko, Modeling and characterisation of cloud dynamics, *Physical Review Letters* 78 (1997) 4297–4300.
[17] S.A. Billings, S. Chen, M.J. Kronenberg, Identification of MIMO nonlinear systems using a forward-regression orthogonal estimator, *International Journal of Control* 49 (1989) 2157–2189.
[18] S.L. Tsyfansky, V.I. Beresnevich, Non-linear vibration method for detection of fatigue cracks in aircraft wings, *Journal of Sound and Vibration* 236 (2000) 49–60.
[19] S. Chen, S.A. Billings, W. Luo, Orthogonal least squares methods and their application to non-linear system identification, *International Journal of Control* 50 (1989) 1873–1896.
[20] S.A. Billings, W.S.F. Voon, Correlation based model validity tests for nonlinear models, *International Journal of Control* 40 (1986) 235–244.
[21] S.A. Billings, Q.M. Zhu, Nonlinear model validation using correlation tests, *International Journal of Control* 60 (1994) 1107–1120.
[22] M. Casdagli, A dynamical systems approach to modelling input–output systems, in: Casdagli, Eubank (Eds.), *Nonlinear Modelling and Forcasting*, Addison-Wesley Publishing Co., Reading, MA, 1992, pp. 266–281.